

# **Radio Emission in Air Showers Measured by LOPES-10 in Coincidence with KASCADE-Grande Observations**

**A.F. Badea, W.D. Apel, T. Asch, L. Bähren,  
K. Bekk, A. Bercuci, M. Bertaina, P.L. Biermann,  
J. Blümer, H. Bozdog, I.M. Brancus, S. Buitink,  
M. Brüggemann, P. Buchholz, H. Butcher,  
A. Chiavassa, F. Cossavella, K. Daumiller,  
F. Di Pierro, P. Doll, R. Engel, H. Falcke,  
H. Gemmeke, P.L. Ghia, R. Glasstetter, C. Grupen,  
A. Haungs, D. Heck, J.R. Hörandel, A. Horneffer,  
T. Huege, K.H. Kampert, Y. Kolotaev, O. Krömer,  
J. Kuijpers, S. Lafebre, H.J. Mathes, H.J. Mayer,  
C. Meurer, J. Milke, B. Mitrica, C. Morello,  
G. Navarra, S. Nehls, A. Nigl, R. Obenland,  
J. Oehlschläger, S. Ostapchenko, S. Over,  
M. Petcu, J. Petrovic, T. Pierog, S. Plewnia,  
H. Rebel, A. Risse, M. Roth, H. Schieler, O. Sima,  
K. Singh, M. Stümpert, G. Toma, G.C. Trincherro,  
H. Ulrich, J. van Buren, W. Walkowiak, A. Weindl,  
J. Wochele, J. Zabierowski, J.A. Zensus,  
D. Zimmermann**

**Institut für Kernphysik  
Institut für Prozessdatenverarbeitung und Elektronik**



# Forschungszentrum Karlsruhe

in der Helmholtz-Gemeinschaft

Wissenschaftliche Berichte

FZKA 7229

## Radio Emission in Air Showers Measured by LOPES-10 in Coincidence with KASCADE-Grande Observations

A.F. Badea<sup>4</sup>, W.D. Apel<sup>5</sup>, T. Asch<sup>1</sup>, L. Bähren<sup>1</sup>, K. Bekk<sup>2</sup>, A. Bercuci<sup>2</sup>, M. Bertina<sup>3</sup>,  
P.L. Biermann<sup>7</sup>, J. Blümer<sup>5</sup>, H. Bozdog<sup>3</sup>, I.M. Brancus<sup>2</sup>, S. Buitink<sup>6</sup>, M. Brüggemann<sup>7</sup>,  
P. Buchholz<sup>7</sup>, H. Butcher<sup>1</sup>, A. Chiavassa<sup>3</sup>, F. Cossavella<sup>8</sup>, K. Daumiller<sup>9</sup>, F. Di Piero<sup>3</sup>, P. Doll,  
R. Engel<sup>5</sup>, H. Falcke<sup>1,4,6</sup>, H. Gemmeke<sup>6</sup>, P.L. Ghia<sup>8</sup>, R. Glasstetter<sup>9</sup>, C. Grupen<sup>7</sup>, A. Haungs,  
D. Heck<sup>6</sup>, J.R. Hörandel<sup>5</sup>, A. Horneffer<sup>6</sup>, T. Huege<sup>9</sup>, K.H. Kampert<sup>7</sup>, Y. Kolotaev<sup>3</sup>, O. Krömer,  
J. Kujipers<sup>6</sup>, S. Lafebre<sup>6</sup>, H.J. Mathes<sup>6</sup>, H.J. Mayer<sup>6</sup>, C. Meurer<sup>7</sup>, J. Milke<sup>2</sup>, B. Mitrica<sup>8</sup>,  
C. Morello<sup>7</sup>, G. Navarra<sup>3</sup>, S. Nehls<sup>6</sup>, A. Nigl<sup>6</sup>, R. Obenland<sup>6</sup>, J. Oehlschläger<sup>10</sup>, S. Ostapchenko,  
S. Over<sup>7</sup>, M. Petcu<sup>2</sup>, J. Petrovic<sup>6</sup>, T. Pierog<sup>5</sup>, S. Plewnia<sup>2</sup>, H. Rebel<sup>8</sup>, A. Risse<sup>10</sup>, M. Roth,  
H. Schieler<sup>2</sup>, O. Sima<sup>2</sup>, K. Singh<sup>6</sup>, M. Stümpert<sup>5</sup>, G. Toma<sup>2</sup>, G.C. Trinchero<sup>8</sup>, H. Ulrich<sup>4</sup>,  
J. van Buren<sup>7</sup>, W. Walkowiak<sup>7</sup>, A. Weindl<sup>7</sup>, J. Wochele<sup>7</sup>, J. Zabierowski<sup>10</sup>, J.A. Zensus<sup>4</sup>,  
D. Zimmermann<sup>7</sup>

Institut für Kernphysik

Institut für Prozessdatenverarbeitung und Elektronik

- <sup>1</sup> ASTRON, 7990 AA Dwingeloo, The Netherlands  
<sup>2</sup> National Institute of Physics and Nuclear Engineering, 7690 Bucharest, Romania  
<sup>3</sup> Dipartimento di Fisica Generale dell'Università, 10125Torino,Italy  
<sup>4</sup> Max-Planck-Institut für Radioastronomie, 53121 Bonn, Germany  
<sup>5</sup> IEKP, Universität Karlsruhe, 76021 Karlsruhe, Germany  
<sup>6</sup> Dpt. Astrophysics, Radboud University, 6525ED Nijmegen, The Netherlands  
<sup>7</sup> Fachbereich Physik, Universität Siegen, 57072 Siegen, Germany  
<sup>8</sup> Istituto di Fisica dello Spazio Interplanetario, INAF, 10133 Torino, Italy  
<sup>9</sup> Fachbereich C - Physik, Universität Wuppertal, 42097 Wuppertal, Germany  
<sup>10</sup> Soltan Institute for Nuclear Studies, 90950 Lodz, Poland

Forschungszentrum Karlsruhe GmbH, Karlsruhe  
2006

Für diesen Bericht behalten wir uns alle Rechte vor

**Forschungszentrum Karlsruhe GmbH**  
Postfach 3640, 76021 Karlsruhe

Mitglied der Hermann von Helmholtz-Gemeinschaft  
Deutscher Forschungszentren (HGF)

ISSN 0947-8620

urn:nbn:de:0005-072296

## Abstract

Data taken during half a year of operation of 10 LOPES antennas (LOPES-10), triggered by EAS observed with KASCADE-Grande have been analysed. We report about the analysis of correlations of radio signals measured by LOPES-10 with extensive air shower events reconstructed by KASCADE-Grande, including shower cores at large distances. The efficiency of detecting radio signals induced by air showers up to distances of 700 m from the shower axis has been investigated. The results are discussed with special emphasis on the effects of the reconstruction accuracy for shower core and arrival direction on the coherence of the measured radio signal. In addition, the correlations of the radio pulse amplitude with the primary cosmic ray energy and with the lateral distance from the shower core are studied.

## Zusammenfassung

### **Messung von Radio Emission in Luftschauern mit LOPES-10 in Koinzidenz mit KASCADE-Grande Beobachtungen**

Daten, die aus einer sechsmonatigen Messkampagne mit durch KASCADE-Grande getriggerten 10 LOPES Radio Antennen (LOPES-10) stammen, wurden analysiert. Wir berichten über eine Analyse der Korrelationen der gemessenen Radiosignale mit Schauergrößen rekonstruiert durch KASCADE-Grande Daten, insbesondere bei Schauern mit großen Abständen der Antennen zum Schauerzentrum. Die Effizienz der Detektion durch Luftschauer induzierter Radiosignale für Schauer mit bis zu 700m Abstand von der Schauerachse wurde untersucht. Die Ergebnisse werden diskutiert, insbesondere unter dem Aspekt der Sensitivität von Schauerobservablen auf die Rekonstruktionsgenauigkeit der Schauergeometrie, d.h. Ort des Schauerzentrums und seiner Ankunftsrichtung. Korrelationen der Stärke des Radiosignals mit der primären Energie des kosmischen Teilchens und dem lateralen Abstand der Antennen zur Schauerachse werden studiert.



## Contents

<b>1</b>	<b>Introduction</b>	<b>1</b>
<b>2</b>	<b>Experimental situation</b>	<b>3</b>
<b>3</b>	<b>Data processing</b>	<b>5</b>
3.1	Selection of candidate events . . . . .	5
3.2	Analysis procedures . . . . .	7
3.3	Coherence of the radio signal . . . . .	9
3.4	Optimized beam-forming . . . . .	11
<b>4</b>	<b>Results</b>	<b>15</b>
4.1	Efficiency of the radio detection . . . . .	15
4.2	Effects of the beam-forming . . . . .	17
4.3	Lateral dependence of the received signal . . . . .	19
4.4	Energy dependence of the received signal . . . . .	21
<b>5</b>	<b>Summary and Outlook</b>	<b>22</b>



## 1 Introduction

In 1962 Askaryan [1] predicted that extensive air showers (EAS) should generate coherent radio emission. A few years later, in 1965, the phenomenon has been experimentally discovered by observing a radio pulse generated during the EAS development at 44 MHz [2]. In the pioneering work of Askaryan coherent Cherenkov radiation of the charge-excess was considered as the process responsible for the EAS radio emission. However, the low matter density in the Earth's Atmosphere and the existence of the Earth's magnetic field allow an alternative process for the origin of the radio signals. In an approach based on coherent geosynchrotron radiation [3], electron-positron pairs generated in the shower development gyrate in the Earth's magnetic field and emit radio pulses by synchrotron emission. Detailed analytical studies [4] and Monte-Carlo simulations [5, 6] predict relevant radio emission at frequencies of 10 to a few hundred MHz. During the shower development the electrons are concentrated in a shower disk, with a thickness of a few meters. This leads to a coherent emission at low frequencies up to 100 MHz, where the wavelength is larger than this thickness. For showers above a certain threshold energy one expects a short, but coherent radio pulse of 10 ns to 100 ns duration with an electric field strength increasing approximately linearly with the primary energy of the cosmic particle inducing the air shower. I.e., one expects a quadratic increase of the received energy of the radio pulse with the primary particle energy [7]. A unified approach, combining the Cherenkov and geosynchrotron mechanisms has also been proposed [8], but the geosynchrotron emission process is expected to be dominant for radio emission during the cosmic ray air shower development [3]. Recently, measurements using the LOPES experiment [9] support these predictions.

Sophisticated experiments, like LOPES [9, 10] or CODALEMA [11, 12] have been deployed to study EAS radio emission. The current efforts attempt to clarify the emission process of the radio signal from EAS and to develop the radio technique as an efficient alternative method for the detection of ultra high energy cosmic rays and of high-energy cosmic neutrinos. The emission is primarily a measure of the total electron and positron content in the shower; hence radio emission is a calorimetric measure indicating the primary energy. Shower thickness and emitted wavelength are in the same order, thus coherence and interference effects are important in this frequency band. As a consequence, the shower geometry is mapped by the wavefront measured by the radio antennas. In addition, in contrast to optical methods, the technique has a high duty cycle, allowing all day observations and, due to low attenuation large solid angle ranges can be observed.

A series of recent papers (e.g. [9, 12, 13, 14, 15, 16]) report about promising experimental results in detecting radio emission in coincidence with air shower events reconstructed by particle detectors. A rather unique opportunity for calibrating and understanding the radio emission in EAS is provided by LOPES, which is located at the site of the KASCADE-Grande experiment [17, 18]. The KASCADE-Grande experiment installed at the Forschungszentrum Karlsruhe is a multi-detector setup which allows high-performance estimations of charged particle EAS observables in the primary energy range of  $10^{14} - 10^{18}$  eV. LOPES-10 is an array of 10 dipole antennas placed inside the particle detector array of KASCADE-Grande. Recently, LOPES-10 was extended with 20 additional antennas to LOPES-30 [19]. These new data are not used in the present analysis.

The present analysis is focused on events with primary energies above  $5 \cdot 10^{16}$  eV which are observed by the KASCADE-Grande experiment and which provide a trigger for LOPES. Special emphasis is put on effects of the applied reconstruction procedures, on detection efficiency, and on features of the measured radio signal dependencies on parameters of the primary cosmic particle such as the primary energy and distance of the antennas from the shower axis. In the present status of our studies there are various shortcomings of

the LOPES-10 measurements, e.g. the lack of an absolute calibration of the radio antennas. The focus of the present paper is to display some general features deduced from a first set of measurements of the LOPES experiment.

## 2 Experimental situation

The KASCADE experiment [20] (Fig. 1, left panel) observes EAS in the primary energy range from 100 TeV to 80 PeV. It enables multi-parameter measurements of a large number of observables of the three main EAS components: electron/ $\gamma$  component, muons, and hadrons. The main detector parts of KASCADE are the field array, the central detector and muon tracking detector. The field array consists of 252 scintillator detector stations and measures the electromagnetic and muonic components with 5 MeV and 230 MeV energy thresholds, respectively. The array is organized in 16 quadratic clusters, where the outer 12 clusters contain electron (unshielded) and muon (shielded) detectors, while the inner four clusters contain electron/ $\gamma$ -detectors, only. It provides basic information about the arrival direction and core position as well as the numbers of muons and electrons ('sizes') of the observed showers. The main trigger of the KASCADE experiment is a multiplicity trigger of the  $e/\gamma$ -detectors in each of the 16 clusters of the array. The muon tracking detector and the central detector provide additional information on shower hadrons and the penetrating muonic component at various energy thresholds, which are not considered in the present analysis.

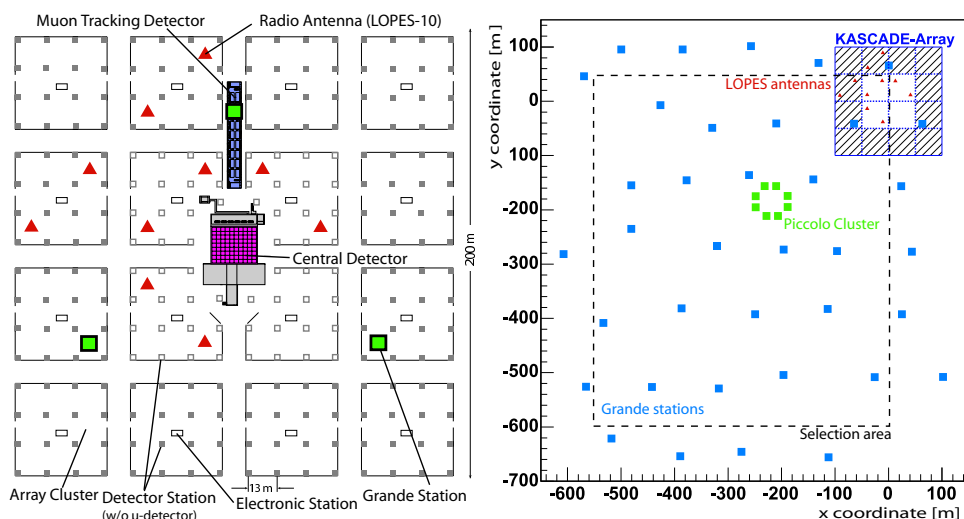


Figure 1: Left panel: The main detector components of the KASCADE experiment: (the 16 clusters of) the field array, the muon tracking detector and the central detector. The location of the 10 LOPES radio antennas is also displayed, as well as three stations of the Grande Array. Right panel: Sketch of the KASCADE-Grande experiment. The dashed line shows the area where showers can be well reconstructed with the Grande array.

KASCADE-Grande [21] is the extension of KASCADE and covers observation of the energy range up to  $10^{18}$  eV. The 37 stations of the Grande array (see Fig. 1, right part) covering an area of approx.  $0.5 \text{ km}^2$  take data in coincidence with KASCADE and allow to reconstruct showers with distances between shower core and the LOPES-10 antennas up to 700 km. The Grande array is triggered by a coincidence of seven neighboring stations. In case of such a trigger event, the KASCADE array detectors are also read out. In addition to the Grande array a compact array, named Piccolo, has been built in order to provide a fast trigger to KASCADE ensuring full joint measurements for showers with cores located far from the KASCADE array.

The present analysis uses data of the Grande array for reconstructing basic shower parameters: location and direction of the shower axis and the shower size.

LOPES [9, 10] is an array of radio antennas, which has been installed on the site of the KASCADE-Grande experiment in order to demonstrate the feasibility of EAS radio measurements. LOPES is based on prototype developments for the Low-Frequency-Array (LOFAR) [22]. In the current status LOPES (**L**Ofar **P**rototyp**E** Station) operates 30 short dipole radio antennas (LOPES-30); the present analysis uses only data of the first 10 antennas forming LOPES-10 (Fig. 1, left part). These 10 antennas are positioned in 5 out of the 16 clusters of KASCADE, 2 of them per cluster. The antennas operate in the frequency range of 40 – 80 MHz and are aligned in east-west direction, i.e. they are sensitive to the linear east-west polarized component of the radiation. The read out window for each antenna is 0.8 ms wide, centered around the trigger received from the KASCADE array. The sampling rate is 80 MHz. The radio data are collected when a trigger is received from the KASCADE array. The logical condition for this LOPES-trigger is at least 10 out of the 16 clusters to be fired. This corresponds to primary energies above  $\approx 10^{16}$  eV; such showers are detected at a rate of  $\approx 2$  per minute. The LOPES-10 experiment is described in more detail in [10, 23].

### 3 Data processing

The LOPES-10 data set is subject of various analyses addressing different scientific questions. With a sample asking for high quality events the proof of principle for detection of air showers in the radio frequency range was made [9]. With events falling inside KASCADE basic correlations with shower parameters were shown [23]. Further interesting features are currently being investigated with a sample of very inclined showers [16] and with a sample of events measured during thunderstorms [24]. Here we report results of an analysis performed by correlating the radio signals measured by LOPES-10 (triggered by the KASCADE array) with EAS events reconstructed by the Grande array. Therefore, these are mainly events with their cores further away from the antennas.

#### 3.1 Selection of candidate events

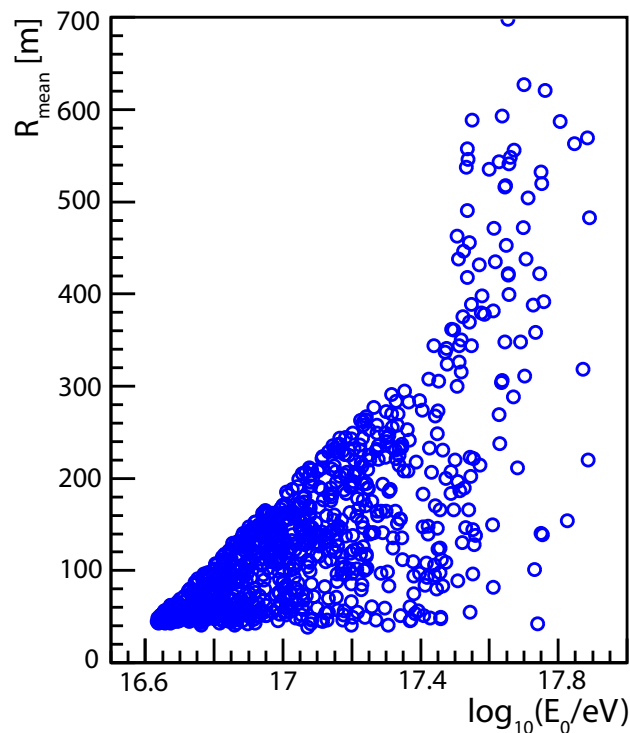


Figure 2: Distribution of the selected candidate events (862 events) on primary energy obtained by Grande and mean distance of the shower axis to the radio antennas.

A sample of 862 candidate events is selected out of five months of LOPES-10 data taken in coincidence with the Grande array. Selection criteria are

- i) coincident measurements of the event by LOPES-10, KASCADE field array which has triggered LOPES, and Grande array;
- ii) a successful reconstruction of the shower observables by the Grande array;
- iii) zenith angle of the shower less than  $50^\circ$ ;
- iv) a geometrical cut to ensure the core position to be inside the fiducial area ( $0.358 \text{ km}^2$ ) of the Grande array, see Fig. 1, right panel;
- v) and, to reduce the amount of data, an energy and distance cut is additionally applied

which is motivated by Allan's formula:

The historical measurements of the 1960s were compiled by Allan [25] with the result that the pulse amplitude per unit bandwidth ( $\varepsilon_v$ ) of the radio signal induced by an EAS is described by the formula:

$$\varepsilon_v = 20 \cdot \left( \frac{E_0}{10^{17} \text{eV}} \right) \cdot \sin \alpha \cdot \cos \theta \cdot \exp \left( -\frac{R}{R_0(v, \theta)} \right) \left[ \frac{\mu\text{V}}{\text{m} \cdot \text{MHz}} \right] \quad (1)$$

with  $E_0$  – primary particle energy in eV,  $\alpha$  – angle between shower axis and the geomagnetic field,  $\theta$  – shower zenith angle,  $R$  – antenna distance to the shower axis, and the scaling radius  $R_0(v, \theta)$ , which is in the range of 30 – 300 m with  $R_0 = 110$  m at 55 MHz and  $\theta < 35^\circ$ .

Compared to  $R$ , for the present analysis the distance  $R_{\text{mean}}$  per event is defined as the mean of the distances between the 10 LOPES antennas and the shower core position (reconstructed by Grande) in shower coordinates, i.e. in planes perpendicular to the axis direction. The cut has been applied as

$$\lg \left( \frac{E_0}{\text{eV}} \right) > \lg \left( \frac{E_{00}}{\text{eV}} \right) + 0.4343 \cdot \frac{R_{\text{mean}}}{R_0} \quad \text{or} \quad \lg \left( \frac{E_0}{\text{eV}} \right) > 17.5 \quad (2)$$

with  $E_{00} = 10^{16.5}$  eV and  $R_0 = 160$  m, i.e. weaker than Allan's scaling with radius. Due to the lack of absolute calibration of the antennas, the threshold primary energy  $E_{00}$  has been chosen based on the results from ref. [9] and data reduction considerations. In this selection there are no conditions on the weather situation at the KASCADE-Grande site, i.e. environmental corrections were not applied. There is a known effect of an amplification of the radio signal during thunderstorms [24], but during the discussed measuring time this affects less than 3% of the selected events.

Fig. 2 shows for these selected events the correlation between primary energy and distance of the antennas to the shower axis. The radius dependent primary energy cut from relation 2 is clearly seen.

### 3.2 Analysis procedures

The Grande array measures the densities and arrival times of the charged particles, from which shower core position and arrival direction are reconstructed. The reconstruction of the shower size  $N_e$  is also based on data of the Grande array, where the lateral distribution of the measured densities is described by a slightly modified NKG-function [26, 27]. The total muon number is obtained by a likelihood fit of the muon densities measured by the KASCADE muon detectors, located in the outer 192 stations of the KASCADE array [28]. For the calculation of the expected particle density in a Grande station a contribution from the previously reconstructed muon lateral distribution function is taken into account. Thus, the free parameters of the global fit to the Grande data per single shower are the core position and the shower direction, as well as the total electron number and the slope parameter of the electron lateral distribution.

In order to select and investigate the candidate events, the primary energy has been roughly estimated from the measured electron and muon numbers by a linear combination where the parameters have been deduced from simulations with fixed energies and five different primary masses by means of a linear regression analysis [27].

This preliminary Grande reconstruction procedures applied to the first year of measurements with Grande lead to accuracies of the shower core position and direction in the order of 8 m and  $0.5^\circ$  with 68% confidence level for simulated proton and iron showers with  $> 50$  PeV primary energy and  $22^\circ$  zenith angle [27]. The energy resolution is estimated to be  $\Delta E/E \approx 30\%$  in the relevant energy range which is sufficient for the following considerations.

The main steps to process the measured LOPES radio raw signals of an individual air shower are the following (for a more detailed description see ref. [23]):

1. Correction of instrumental delays: The phase stability of the antenna system is monitored and time delay calibration values are obtained by monitoring the relative phases of a TV transmitter in the measured frequency band.
2. Gain correction: The amplification or attenuation factors of all electronic components in the signal chain have been measured in a laboratory environment. The values obtained are combined to a frequency dependent gain factor, which the data are corrected for.
3. Suppression of narrow band radio frequency interference (RFI): The narrow band RFI occupies only a few channels in frequency space, while a short time pulse (e.g. from an EAS) is spread over all frequency channels. So, by flagging the channels with RFI the background is significantly reduced without affecting the air shower pulse significantly. Remaining antennas with high noise are flagged for the further procedures.
4. Digital beam forming: The beam forming consists of two steps: First, a time shift of the data according to the given direction is done and then the combination of the data is performed calculating the resulting beam from all antennas. The geometrical delay (in addition to the instrumental delay corrections) by which the data is shifted, is the time difference of the pulse coming from the given direction to reach the position of the corresponding antenna compared to the reference position. This shift is done by multiplying a phase gradient in the frequency domain before transforming the data back to the time domain.

To form the beam from the time shifted data, the data from each pair of antennas is multiplied pixel by pixel, the resulting values are averaged, and then the square

root is taken while preserving the sign. We call this the cross-correlation beam or CC-beam:

$$CC(t) = \text{sign}(S(t)) \sqrt{\frac{1}{N_p} |S(t)|} \quad \text{with} \quad S(t) = \sum_{i \neq j}^N s_i(t) \cdot s_j(t) \quad , \quad (3)$$

with  $N$  the number of antennas,  $N_p$  the number of antenna pairs,  $s_i(t)$  the field strength of antenna  $i$ , and  $t$  the time pixel index. The advantage of the CC-beam is that a peak from a coherent pulse always has a positive sign, where peaks from incoherent pulses can also have a negative sign.

The radio wavefront of an air shower is not expected to arrive as a plane wave on the ground, it should have some curvature. During the reconstruction procedures the radius of this curvature is taken into account by iterating a free parameter until the CC-beam is maximal. To some extent, however, the obtained value of this free parameter is degenerated by the uncertainties in the shower direction and due to the fact that the signal is generated in an extended and not point-like source.

5. Quantification of the radio parameters: Due to the filtering of low and high frequencies, the response of the analog electronics to a short pulse is an oscillation over a short time. Sampling such a signal with an ADC gives a certain fine structure inside the pulse that is not part of the original pulse but is caused mainly by the filter. To suppress this fine structure the data is smoothed by block averaging over 3 samples in the time domain. Although the shape of the resulting pulse (CC-beam) is not really Gaussian, fitting a Gaussian to the smoothed data gives a robust value for the peak strength. The value for the peak strength that is used in the present analysis is the height of this Gaussian. The error of the fit results give also a first estimate of the uncertainty of this parameter.

The final parameters for the reconstructed air showers are therefore the peak height of the obtained pulse per unit bandwidth  $\epsilon_v$ , a value for the so called ‘radius of curvature’, and the distance of the antennas to the shower axis  $R_{\text{mean}}$  as defined in the previous section. The obtained value for  $\epsilon_v$ , which is the measured amplitude divided by the effective bandwidth, will be given in units of [ $\mu\text{V}/\text{m}\cdot\text{MHz}$ ], but has to be multiplied by an unknown quantification factor  $A$  due to the lack of an absolute calibration. The current best estimate for  $A$  is approximately seven [29].

6. Identification of good events: Not every selected air shower is accompanied by a radio pulse which is detectable by LOPES. There can also be an incoherent noise peak which is as high as a peak induced by the air shower, even in the formed beam. One can therefore not select events with air shower pulses just by the height of the fitted Gaussian, but has to classify events in a further step. The criteria for this selection are: existence of a pulse, coherence of the pulse, expected position of the pulse in time, and an approximately uniform pulse height in all antennas. Up to now these criteria are verified by hand.

### 3.3 Coherence of the radio signal

A crucial element of the detection method is the digital beam-forming which allows to place a beam in the direction of the cosmic ray event. This is possible because the phase

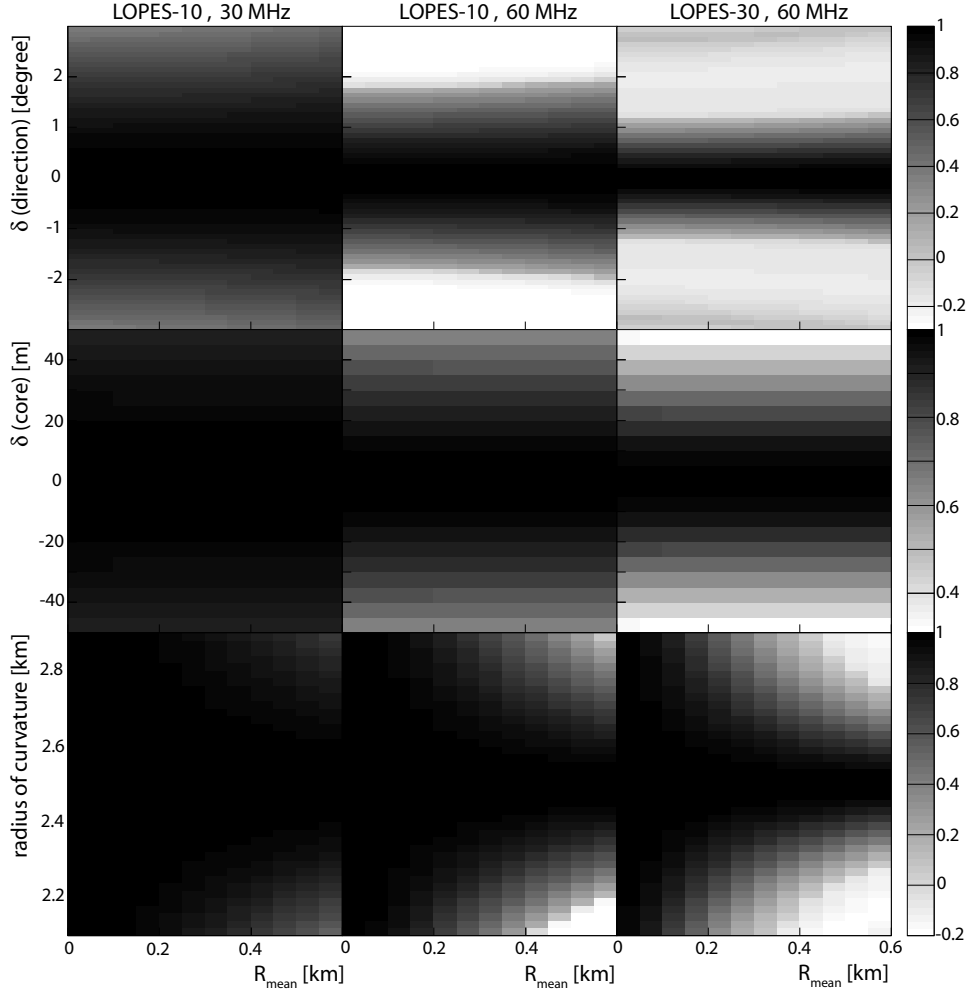


Figure 3: Analytically estimated sensitivity of the (cross correlation) CC-beam to the error of the shower direction  $\delta(\text{direction})$ , the shower core position  $\delta(\text{core})$ , and the radius of curvature of the radio front in dependence of  $R_{\text{mean}}$  for the LOPES-10 configuration (assuming a monochromatic point source emitting at 30MHz and 60MHz) and LOPES-30 configuration (point source emitting at 60MHz).

information of the radio waves is preserved by the digital receiver and the cosmic ray produces a coherent pulse. The method is also very effective in suppressing interference from the particle detectors which radiate incoherently. In addition to characteristics of the primary particle inducing the air shower like primary energy and mass, the observed radio signal is expected to be sensitive also to the core position, to the shower direction, and to the radius of curvature of the emitted wave front. To investigate the intrinsic capabilities of the beam-forming in case of LOPES a simple simulation has been performed based on analytical calculations.

For a monochromatic point source radiating at 30 MHz or 60 MHz, placed at a position of 2.5 km along the vertical shower axis from the ground, the sensitivity of the CC-beam estimator (eqn. 3) has been calculated.

Fig. 3 gives an impression of the relation of the CC-beam to the shower direction, the shower core position and the radius of curvature of the radio front for the LOPES-10, and for comparison, also for the LOPES-30 configuration. The z-axis in the figure is normalized to the value of the CC-beam estimator in case of ‘perfect’ coherence, i.e. no uncertainties in the position of the radio point source ( $\delta(\text{direction})=0$ ,  $\delta(\text{core})=0$ , and radius of curvature= 2.5 km). Only one parameter is varied at a time, where the other two are set to the true value. The performed beam-forming can lead to so-called side lobes, which are a known effect in interferometry, and are also visible in Fig. 3 by the anew increasing values after the minima.

The middle column of the figure shows results obtained for the geometrical layout of LOPES-10. It shows that one loses (z-value is decreased by 20%) coherence if the start parameters for the CC-beam estimation in the direction are reconstructed with an error of more than  $0.8^\circ$ , and the core position with an error of more than 25 m, respectively. In contrast to direction and core, the distance of the shower axis from the antennas is relevant for the radius of curvature. The further away from the axis, the more important the precision of the radius parameter becomes. On the other hand the results shown in Fig. 3 can be interpreted as the intrinsic resolution of the antenna system, i.e. LOPES-10 has a limit in direction resolution of  $0.8^\circ$  and in core resolution of 25 m, and the further away the shower axis is the better the resolution gets as the uncertainty in the radius estimate decreases.

The sensitivity of the antenna system working in coincidence with the particle array depends less critically on the input parameters if lower frequencies (left column) are considered due to a better coherence, and slightly more critically if more antennas are involved (right column). The latter is caused only due to the wider spread of the antennas, i.e. a longer baseline. The intrinsic resolution (using radio information alone) would improve with more antennas. The figure shows also that going to lower frequencies the better coherence improves the primary energy estimation, where measuring at high frequencies improves the reconstruction accuracy of the shower geometry.

### 3.4 Optimized beam-forming

As shown in Fig. 3, the procedure of time shifting the radio signals is relatively safe when the shower parameters for core and axis are reconstructed with high accuracy, i.e. provided by the reconstruction of data taken with the original KASCADE field array. Due to the high sampling area the accuracy of the core position and direction is good enough to obtain good coherence of the radio signals. Of course, this is valid only for showers with cores inside KASCADE, i.e. distance between antennas and shower axis less than 0.2km, and for not too energetic showers which may lead to saturation and therefore to a reduction of the reconstruction accuracy of KASCADE.

A shower reconstruction using data from the Grande array is required for shower cores outside KASCADE. The Grande stations cannot assure an accuracy comparable with the original KASCADE array. This leads to events whose reconstructed radio signals do not fulfill the requirements to qualify as detected in the radio channel. Therefore, a so-called optimized beam-forming is performed, which searches for maximum coherence by varying the core and the direction around the values provided by the Grande reconstruction. I.e., the whole data reconstruction procedures for the antennas - as described above - are repeated 50 times per shower, where the core and direction are randomly chosen inside the parameter space given by the KASCADE-Grande reconstruction accuracy. The effect on radio detection by such an optimized beam-forming will be illustrated by a few examples, where their geometrical situation is displayed in Fig. 4.

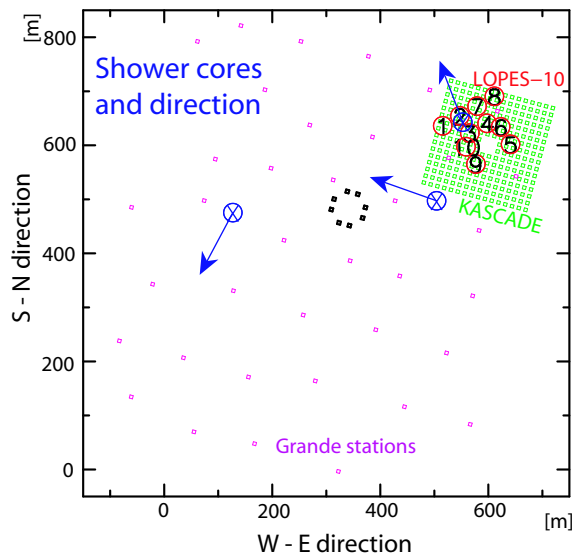


Figure 4: Shower core positions of three radio events. The arrows point towards the incoming direction of the shower as reconstructed by Grande. The events correspond to the data displayed in Figs. 5, 6, and 7; their zenith angles are reconstructed to  $40^\circ$ ,  $34^\circ$ , and  $33^\circ$ , respectively.

Fig. 5 shows the result of such an optimized beam-forming compared with results of the initial beam-forming for an event with a medium distance between shower axis and radio antennas. An increase of 50% is seen in the CC-beam estimator after the optimized

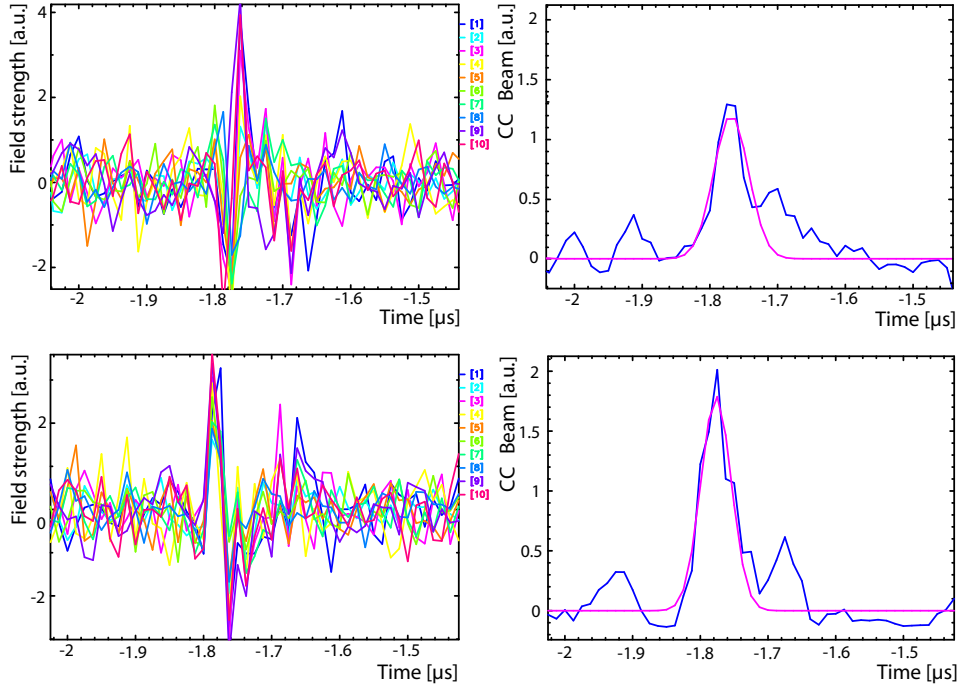


Figure 5: EAS radio event at medium distance. Upper panels: Signals of the individual antennas and result of the beam-forming based on shower observables reconstructed by Grande; Lower panels: Signals of the individual antennas and result of the optimized beam-forming in order to maximize the radio coherence.

beam-forming. In the upper part of the figure the raw time-series of the 10 antennas and the corresponding CC-beam including the fit to obtain the radio parameters are shown. The lower part shows the same event by choosing those starting parameters for the beam-forming which led to the maximum coherence, i.e. the highest radio pulse. Table 1 gives the shower parameter values and their changes after achieving maximum coherence.

Table 1: Shower observables reconstructed by Grande alone and obtained after optimized beam-forming of LOPES-10 data for the EAS radio events displayed in Figs. 5, 6, and 7. For the event from Fig. 6 also the KASCADE obtained values are given. The values of the shower core are given in KASCADE-Grande coordinates (Fig. 1), the mean distance is the mean of the distances from the shower axis to the individual antennas.

Shower Observable	EAS from Fig. 5		EAS from Fig. 6			EAS from Fig. 7	
	Grande	LOPES	Grande	LOPES	KASCADE	Grande	LOPES
$\phi$	289.5°	292.2°	338.9°	337.8°	336.7°	208.1°	203.3°
$\theta$	41.1°	40.6°	36.8°	34.0°	33.8°	40.8°	43.3°
$X_{\text{core}}/\text{m}$	-66.0	-64.4	-60.6	-48.4	-44.0	-427.0	-412.2
$Y_{\text{core}}/\text{m}$	-124.0	-123.0	28.1	37.2	43.5	-248.8	-235.7
$R_{\text{mean}}/\text{m}$	149.8		48.3			399.9	
$\log_{10}(E_0/\text{GeV})$	8.6		8.4			8.7	

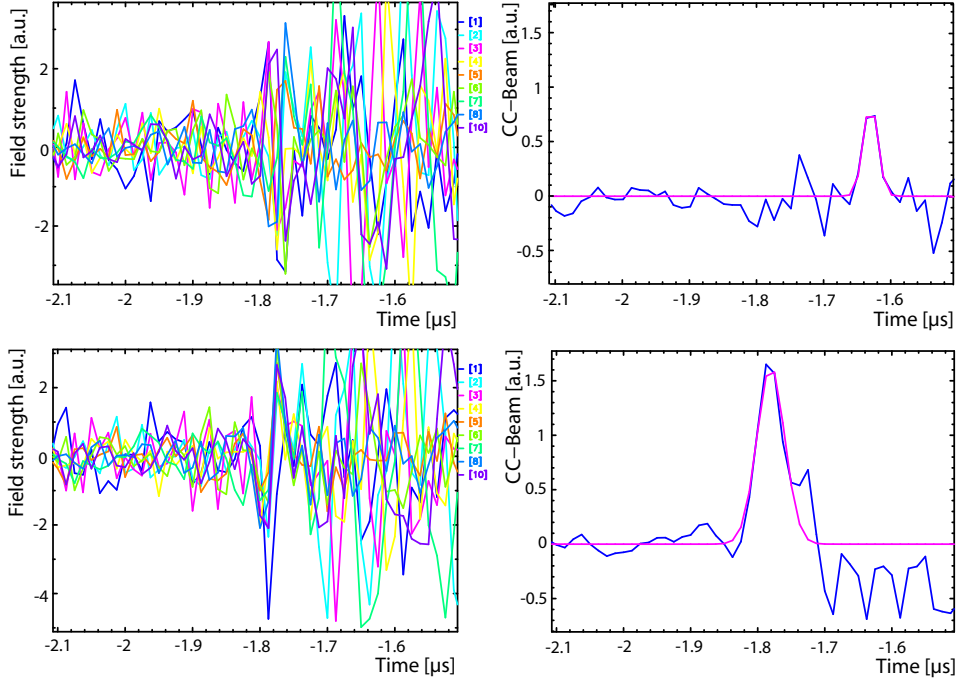


Figure 6: EAS radio event at short distance. Upper panels: Signals of the individual antennas and result of the beam-forming based on shower observables reconstructed by Grande; Lower panels: Signals of the individual antennas and result of the optimized beam-forming in order to maximize the radio coherence.

Another example of the improvement reached in coherence by applying the optimized beam-forming procedure is displayed in Fig. 6, which shows radio detection at a short distance. Due to the small distance to the shower axis, the particle density detected by the KASCADE array is relatively high inducing a lot of radio noise (incoherent signals, but still visible in the CC-beam estimation). After optimized beam-forming these incoherent signals cancel out and the CC-beam value can become even negative. The results displayed in the upper panels of Fig. 6 finds a CC-Beam peak not at the expected time, which is not associated with the EAS coherent radio signal but is generated purely by the incoherent radio signals coming from the KASCADE particle detectors. Therefore, it is very important that the CC-Beam peak appears in the expected time range.

Because this event is hitting the KASCADE array, it can also be reconstructed with KASCADE data independent of the Grande reconstruction, but with better accuracy. These values are also given in Table 1. It is obvious that after the optimized beam-forming the two independently estimated parameter sets are in better agreement.

Finally, Fig. 7 shows an example of a distant event with a clear radio signal. The mean distance from the antennas to the shower axis is around 400m. This radio event is seen in both cases, after the initial beam-forming and also after the optimized beam-forming procedures. But, again a better estimation of the signal (30% increase in the CC-Beam estimator) is assured by small changes of the starting parameters (see Tab. 1). For the reconstruction of this event an expected time shift, calculated by use of the known core distance, has to be taken into account to find the correct coherent peak. Such shifts serve as an additional constraint on the analysis procedure, especially for events with large distance to the antennas.

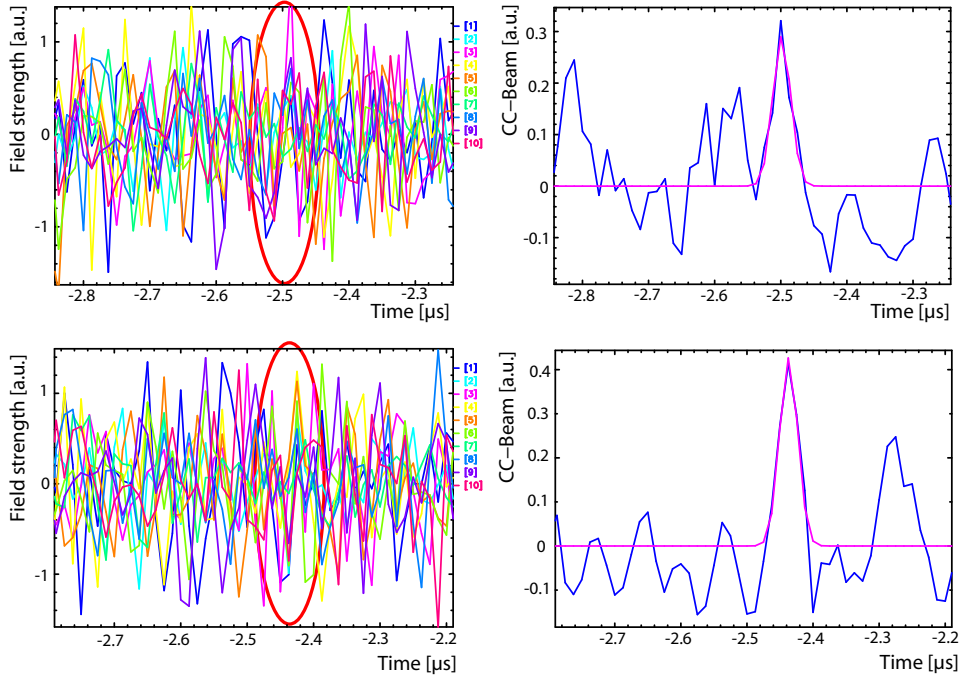


Figure 7: EAS radio event at large distance. Upper panels: Signals of the individual antennas and result of the beam-forming based on shower observables reconstructed by Grande; Lower panels: Signals of the individual antennas and result of the optimized beam-forming in order to maximize the radio coherence.

Table 1 contains in addition to primary energy and mean distance also the azimuthal angle  $\phi$ , zenith angle  $\theta$ ,  $X_{core}$ , and  $Y_{core}$  reconstructed by Grande as well as the corresponding values as obtained after maximizing the radio coherence for the events displayed in Figs. 5 and 6 and 7. Small shifts in shower core and direction (inside the Grande resolution) assure an almost perfect coherence of the radio signal.

As the second example (Fig. 6) shows, the optimized beam-forming gives the possibility to improve the accuracy of shower parameters by including the radio information in the reconstruction of the shower with Grande. This concerns the core position and shower direction directly, then iteratively with the new values the reconstruction of the shower sizes and therefore also the primary energy and mass estimation. This example represents one out of 10 events with the core inside KASCADE and an improved coherence by applying the optimization procedure. For all cases the geometrical values of the showers obtained after the optimization, i.e. with LOPES information, are closer to the KASCADE obtained values than by using Grande data alone. This important feature of radio measurements will be a main direction of further studies with LOPES in the next years.

## 4 Results

### 4.1 Efficiency of the radio detection

Fig. 8 displays the efficiency of detecting radio signals, i.e. in each bin the fraction of the candidates events (Fig. 2) is shown which survive as EAS radio detected events. The left part of the figure displays the efficiency obtained by using the beam-forming procedure based on the values provided by the Grande reconstruction of shower core and direction, only. As shown in the previous section, the search for a coherent radio signal is very sensitive to the accuracies of reconstructing core position and shower direction. Due to the insufficient resolution of Grande, a lot of radio events fail in the CC-beam reconstruction. After searching for maximum coherence by varying the core position and direction (i.e. optimized beam-forming), the efficiency is as displayed in the right part of Fig. 8, where the number of detected radio events increases from 101 to 372 out of 862 candidate events.

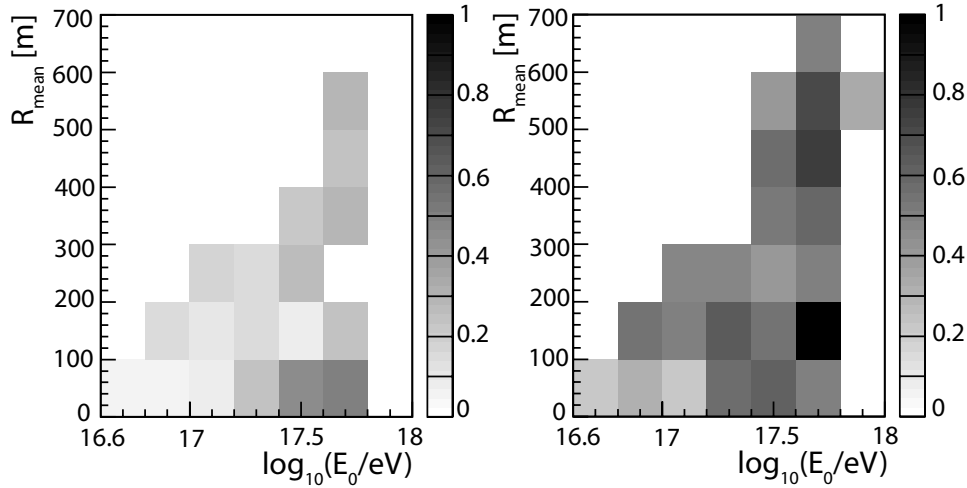


Figure 8: Left panel: Efficiency of the radio detection for the initial beam-forming (in total 101 of the 862 selected events); Right panel: Efficiency of the radio detection after the optimized beam-forming (372 out of 862 events).

The very small efficiencies visible in the lower-left part of Fig. 8 are caused by low primary energies as well as due to the high radio noise coming from the KASCADE particle detectors. For short distances from the shower axis such high particle densities occur giving a bias in the beam-forming caused by accidental coherence in the noise pattern (see also example in Fig. 6). The best efficiency is reached for showers with high energy but not too large distances, where the signal is strong but the noise from the particle detectors weak.

One of the most interesting results of the current analysis is the presence of clear EAS radio events at more than 500m distance from the shower axis for primary energies below  $10^{18}$  eV. Concerning the overall detection threshold an increasing efficiency with increasing primary energy reaching approximately 60% for primary energies above  $2 \cdot 10^{17}$  eV is obtained with LOPES-10 (Fig. 9).

Other shower parameters have to be investigated in more detail to find reasons for efficiencies below 50%, even after applying the optimized beam-forming procedures. Here the

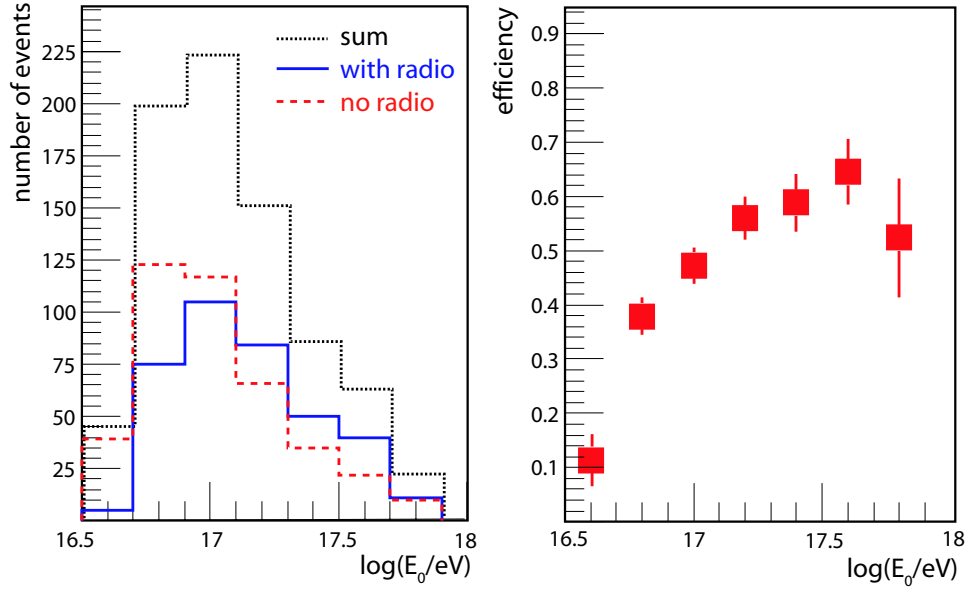


Figure 9: Left panel: Energy distribution of the selected events, the events with detected radio signal (372 EAS) and the events without detected radio signal (490 EAS). Right panel: Efficiency for radio detection versus primary energy.

direction of the shower axis plays the main role: By simulations [6] it is expected that the emission mechanism in the atmosphere and therefore also the radio signal strength depends on the zenith, on the azimuth, and as a consequence on the geomagnetic angle. The latter is the angle between the shower axis and the direction of the geomagnetic field. Indeed, detailed analyses of LOPES data have shown [9, 23, 16] that there are preferred directions for enhanced radio signals, or vice versa there is no radio signal detection for specific shower conditions, especially at the detection threshold. An aggravating circumstance for the interpretation of these dependences is the fact that with LOPES-10 only one polarization direction is measured, which leads also to some specific dependencies and missing of emission detection.

For the present analysis there is also a selection bias: For large distances mainly showers with small zenith angles are selected due to the fact that the trigger condition requires high particle densities inside the KASCADE array, which is located in a corner of the Grande array. Small zenith angles lead to higher particle densities at KASCADE for same primary energy, and therefore to a weaker signal to noise ratio in the antennas.

In addition, the probability to detect an air shower in radio might also be influenced by variations of the background noise due to weather conditions or day-night effects in the human dominated environment of LOPES.

## 4.2 Effects of the beam-forming

Fig. 10 shows the change in direction and core position for all events which are identified as radio event after the optimized beam-forming, but not by the first beam-forming. For the angle we obtain a mean shift of  $2.3^\circ$ , which is still reasonable if we assume an uncertainty of roughly  $1^\circ$  for the present state of Grande reconstruction [27] and also  $\approx 1^\circ$  for LOPES-10 [9]. The mean shift in core position, displayed in Fig. 10 (right panel) is 15 m which is

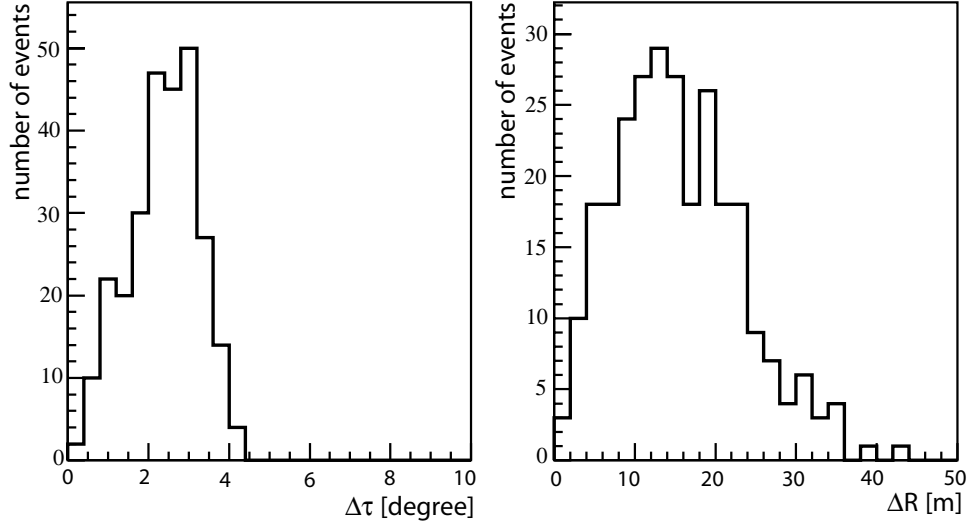


Figure 10: Difference in angle and core position between the results of the Grande reconstruction and the values derived with optimized beam-forming (for the 271 events in which a change occurred).

also not far off from the reconstruction uncertainties. However, we recognize a systematic shift of the cores in direction to the antenna center (not shown here explicitly). Probably this systematic effect is connected with the so-called radius of curvature of the wave front as introduced in the fitting procedure. It appears that for the selected sample this radius parameter decreases with increasing distance to the shower axis [15]. Comparing this result with the studies shown in Fig. 3, one can interpret it as confirmation for an increasing sensitivity to this parameter with increasing distance. In Fig. 3 an increased sensitivity of the CC-Beam estimator with respect to the radius of curvature for large distances is shown. Although, the calculations in Fig. 3 have been made for a point source the trend should be quite similar for an extended source.

In case of a point source, the obtained radius parameter should give hints to the position of the source (height above observation level), but a couple of reasons smear out this information: First, it is not clear where the dominant part of the radio emission comes from. There is a strong emission at the shower maximum due to the maximum number of particles. At later stages there are less particles but the emission happens closer to the observer, what can compensate the  $1/R$  attenuation of the generated field strength at shower maximum. Second, the correlations can also arise by effects of the applied reconstruction procedures. In the beam-forming procedures a spherical radio front is adopted, in other words the radio emission is assumed to be produced by a point source, but in reality the source is extended. In addition the procedure of calculating the CC-beam may suffer from systematic effects, e.g. the relevant time shifts are done by assuming same widths of the

radio pulses, which could, however, vary from antenna to antenna due to fluctuations of the behavior of the electronic units. Third, in the current configuration LOPES is triggered by the KASCADE particle detectors which slightly bias the selection, because the radio antennas are in the same region (i.e. solid angle seen from the EAS) as the field detectors generating the trigger, which may have an influence if the radio emission or particle production in the shower is not axis-symmetric.

In summary, with the available statistics and still partly preliminary calibrations for both the Grande and LOPES detectors, it would be premature to investigate any possible systematic shift between the ‘radio’ and the ‘particle’ axis of the shower. In the future also more detailed simulations will provide appropriate shapes for the radio front, which will help to understand the observed systematics.

### 4.3 Lateral dependence of the received signal

Fig. 11 shows the radio pulse strength versus mean distance and versus estimated energy for all 372 radio detected events. No clear correlation is seen, neither between the distance and the radio pulse amplitude nor between the primary energy and the radio signal. These are expected behaviors due to the large interconnected dependence of the signal on these two parameters.

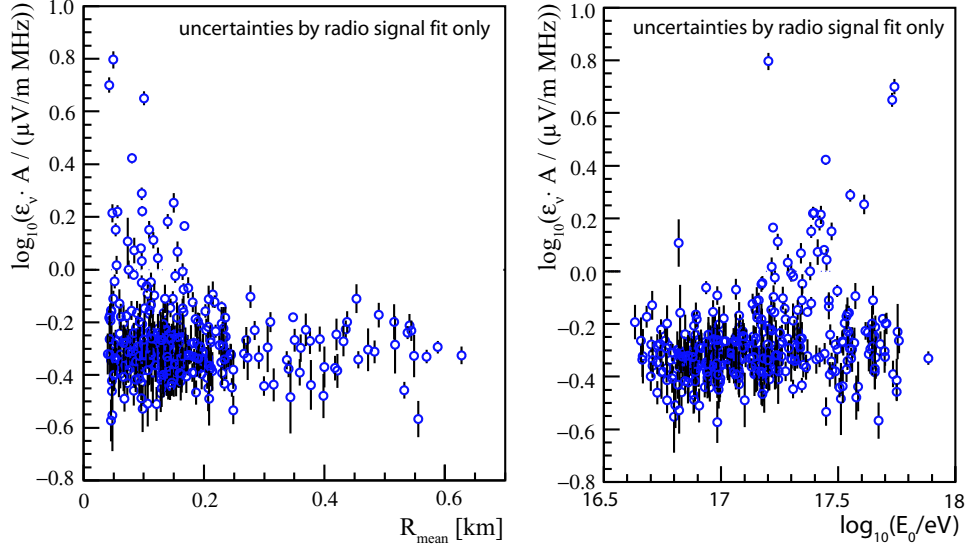


Figure 11: Left panel: Radio signal versus the mean distance of the shower axis to the radio antenna system. Right panel: Radio signal versus the primary energy. The value  $A$  describes an unknown factor due to the missing absolute calibration of the antennas. The error bars denote the uncertainties of the radio signal fit to the CC-beam pulse height only, and no systematic uncertainties are included.

After linear scaling of the pulse amplitude  $\epsilon_v$  with the primary energy estimated by KASCADE-Grande a clear correlation with the distance is found (Fig. 12). The functional form of this dependence and also the lateral scaling parameter is of high interest for the further development of the radio detection technique. Following Allan's formula an exponential behavior with a scaling parameter of  $R_0 = 110\text{m}$  is expected (eqn.1 and [25]) for vertical showers. Such an exponential dependence of signal to distance is also expected by detailed simulations of the geosynchrotron effect with a scaling radius of  $\sim 100$  to  $\sim 800\text{m}$ , increasing with increasing zenith angle [6]. The CODALEMA experiment does also support such a dependence by a preliminary analysis of a few events ( $R_0$  of a few hundred meters) [30]. Fitting the present data set (Fig. 12) explicitly assuming an exponential function,  $R_0$  results to  $230 \pm 51\text{m}$ , i.e. somewhat larger than Allan's suggestion which is also drawn in Fig. 12. One has to note that the initially introduced energy dependent selection cut (eqn. 2), and the large noise contribution (weak signal) for large distances certainly bias the obtained result on the lateral scaling parameter towards a flatter slope. In addition, the selection cut as well as the different definition of  $R_{\text{mean}}$  compared to the definition of the distance  $R$  used in Allan's formula surely distort the obtained scaling parameter.

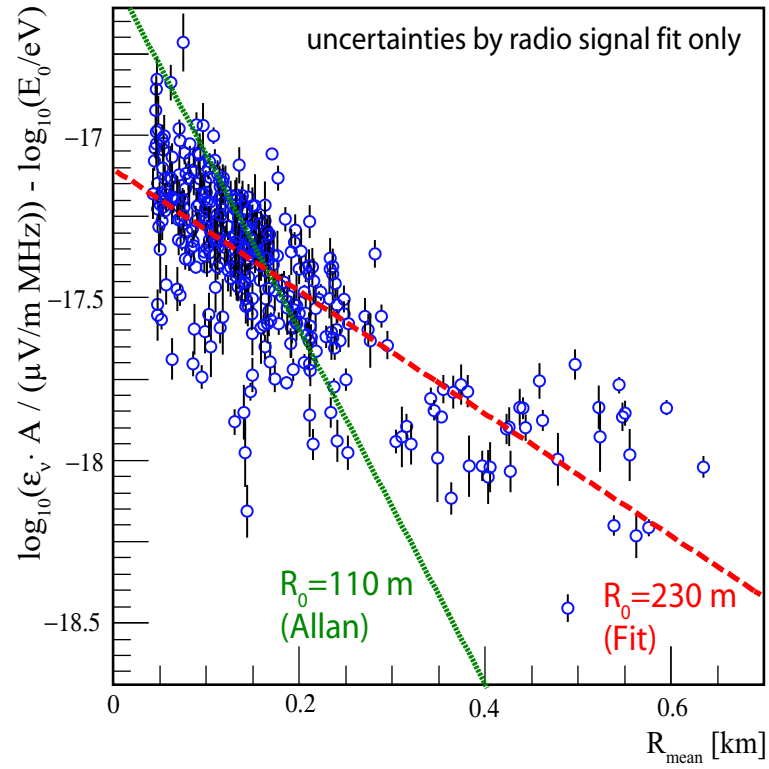


Figure 12: Correlation of the pulse height corrected for primary energy with the mean distance of the shower axis to the radio antenna system. The lines show results of fits with an exponential function with two free parameters (fit) and with one free parameter (Allan, fixed scaling radius), respectively.

#### 4.4 Energy dependence of the received signal

In Fig. 13 the pulse amplitudes are now scaled according to the exponential radial factor obtained by the fit described in the previous section, without the prior energy correction. Now, a clear correlation between the radio field strength and the primary energy is found.

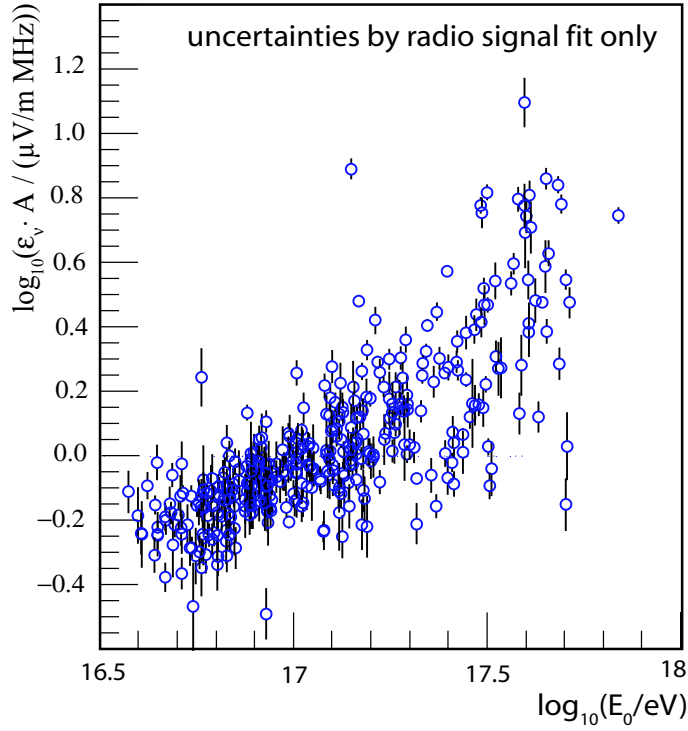


Figure 13: Correlation of the pulse height (corrected for the lateral mean distance of the shower axis to the radio antenna system) with the primary energy of the showers. No correction for the dependence on the geomagnetic angle, on the zenith angle, or the azimuth angle are applied.

By scaling in addition subsequently with the angle to the geomagnetic field, the azimuth, and the zenith angles, an even stronger correlation with less fluctuations would be expected. Due to the low statistics and the discussed systematic uncertainties of the experimental configuration as well as the efficiency behaviour of the detection, these steps are omitted in the current phase of the analysis. Consequently, we omit also to perform a fit to the presented data. Nevertheless, the shown correlation supports the expectation that the field strength  $\epsilon_v$  increases by a power-law with an index close to one with the primary energy, i.e. that the received energy of the radio signal increases quadratically with the primary energy of the cosmic rays. The index of this power-law exactly one would serve as a proof of the coherence of the radio emission during the shower development.

## 5 Summary and Outlook

A combined data analysis correlating the radio signals measured by LOPES-10 with extensive air shower events reconstructed by KASCADE-Grande was performed. The analyzed showers had their axis in up to 700m distance from the antenna array and in the primary energy range of  $10^{16.5} - 10^{18}$  eV. Some general dependences of the measured radio signal on certain shower parameters were discussed. Missing statistics and experimental deficiencies hamper more detailed investigations in this early stage of air shower radio detection experiments. Nevertheless, the presented first analysis led to some interesting results which can be summarized as follows:

- The most crucial element of radio detection is finding the coherence of the radio pulses. The coherence itself is very sensitive to the shower direction and shower core position. On the one hand, very small fluctuations in the shower observables reconstructed by Grande translate into large fluctuations in the estimated radio pulse amplitude. On the other hand, by maximizing the radio coherence, improved estimations of the core and direction parameters can be performed. The maximization of the radio coherence (optimized beam-forming) therefore plays a key role in detecting EAS radio signals. It increases the efficiency of the radio detection and improves the quality of investigations of the correlations between the intensity of the radio signal and the other EAS parameters. Only then a comparison between simulated and reconstructed electric fields will be valuable (including an absolute calibration of the antennas as it will be the case for LOPES-30).
- LOPES-10 is able to detect radio signals (at 40 – 80MHz) induced by extensive air showers even at distances of more than 500m from the shower axis for primary energies above  $10^{17}$  eV.
- The dependence of the radio signal strength on the distance of the antennas to the shower axis can be described by an exponential function with a scaling radius in the order of a few hundred meters, as expected by simulations of the geosynchrotron mechanism.
- For LOPES-10 an energy detection threshold for primary energies below  $10^{17}$  eV was found, which is remarkably low considering the noisy environment at the experimental site and the missing second polarization measurement.
- After scaling with the lateral dependence, a nearly quadratical increase of the received energy of the radio pulse with the primary energy could be obtained, confirming the coherent character of the emission mechanism during the shower development.
- Both lateral and energy dependence of the radio signal are in agreement with the suggestions of Allan, given in 1971 by a compilation of early data of shower radio measurements.

With the measurements of LOPES-10 it could be shown that the radio signal in air showers depends on various parameters: The primary energy, the distance to the shower axis, and the direction of the shower axis. The latter includes the angle respective to the geomagnetic field, the zenith angle of the axis, as well as the azimuth angle of the arriving shower, but these were not discussed in the present analysis. Additionally, for all dependences the polarization direction of the measurements plays a role, which was also not investigated with LOPES-10. In the present analysis first hints to the lateral structure and to the energy dependence of the radio signal could be derived. With data of the current extension, LOPES-30, consisting of thirty absolute calibrated antennas and the possibility

of an additional trigger by Grande, a larger baseline and higher statistics in the measurements will be available. With LOPES-30 one can also use independent subsets of antennas for the CC-beam estimate, and would then have the possibility to estimate the electric field several times, which allows a reconstruction of the lateral extension of the radio emission per single air shower. Additionally, polarization measurements will be performed with LOPES-30. With that data set LOPES-30 is expected to calibrate the radio emission in air showers in the primary energy range from  $10^{16}$  eV to  $10^{18}$  eV.

*The authors would like to thank the engineering and technical staffs of the involved institutes. They contribute with enthusiasm and commitment to the success of the experiment. The corresponding author (A.F.B.) acknowledges very useful discussions with Dr. Tom Thouw. LOPES was supported by the German Federal Ministry of Education and Research (Verbundforschung Astroteilchenphysik). This work is part of the research programme of the Stichting voor Fundamenteel Onderzoek der Materie (FOM), which is financially supported by the Nederlandse Organisatie voor Wetenschappelijk Onderzoek (NWO). The KASCADE-Grande experiment is supported by the German Federal Ministry of Education and Research, the MIUR of Italy, the Polish State Committee for Scientific Research (KBN grant 1 P03B03926 for 2004-06) and the Romanian National Academy for Science, Research and Technology.*

## References

- [1] G.A. Askaryan, Soviet Phys. JETP 14 (1962) 441.
- [2] J.V. Jelley et al., Nature 205 (1965) 237.
- [3] H. Falcke and P.W. Gorham, Astropart. Phys. 19 (2003) 477.
- [4] T. Huege and H. Falcke, Astron. and Astroph. 412 (2003) 19.
- [5] T. Huege and H. Falcke, Astron. and Astroph. 430 (2005) 779.
- [6] T. Huege and H. Falcke, Astropart. Phys. 24 (2005) 116.
- [7] S.N. Vernov et al., Can. J. Phys. 46 (1968) 241.
- [8] R. Engel, N.N. Kalmykov and A.A. Konstantinov, "Simulation of Cherenkov and Synchrotron Radio Emission in EAS", Proc. 29<sup>th</sup> ICRC, Pune, India, Tata Institute of Fundamental Research, eds. B. S. Acharya et al., Vol. 6 (2005) 9.
- [9] H. Falcke et al. - LOPES collaboration, Nature 435 (2005) 313.
- [10] A. Horneffer et al. - LOPES collaboration, Proc. SPIE 5500-21, Astronomical Telescopes and Instrumentation Symposium, Glasgow, Scotland, 21-25 Jun 2004, astro-ph/0409641 (2004).
- [11] O. Ravel et al. - CODALEMA collaboration, Nucl. Instr. Meth. A 518 (2004) 213.
- [12] D. Ardouin et al. - CODALEMA collaboration, "Radio detection of Extensive Air Showers with CODALEMA", Proc. 29<sup>th</sup> ICRC, Pune, India, Tata Institute of Fundamental Research, eds. B. S. Acharya et al., Vol. 8 (2005) 331.
- [13] A. Horneffer et al. - LOPES collaboration, "Detection of radio pulses from extensive air showers", Proc. 29<sup>th</sup> ICRC, Pune, India, Tata Institute of Fundamental Research, eds. B. S. Acharya et al., Vol. 6 (2005) 285.
- [14] A.F. Badea et al. - LOPES collaboration, "First determination of the reconstruction resolution of an EAS radio detector", Proc. 29<sup>th</sup> ICRC, Pune, India, Tata Institute of Fundamental Research, eds. B. S. Acharya et al., Vol. 6 (2005) 273.
- [15] A.F. Badea et al. - LOPES collaboration, "Remote event analyses of LOPES-10", Proc. 29<sup>th</sup> ICRC, Pune, India, Tata Institute of Fundamental Research, eds. B. S. Acharya et al., Vol. 6 (2005) 277.
- [16] J. Petrovic et al. - LOPES collaboration, "Radio emission of highly inclined cosmic ray air showers measured with LOPES", Proc. 29<sup>th</sup> ICRC, Pune, India, Tata Institute of Fundamental Research, eds. B. S. Acharya et al., Vol. 6 (2005) 337.
- [17] G. Navarra et al. - KASCADE-Grande collaboration, Nucl. Instr. Meth. A 518 (2004) 207.
- [18] A. Haungs et al. - KASCADE-Grande collaboration, Proc. of 28<sup>th</sup> ICRC, Tsukuba, Japan, Universal AScademy press Tokyo, eds. T. Kajita et al., (2003) p.985.
- [19] S. Nehls et al. - LOPES collaboration, "LOPES-30: A digital antenna array for measuring high-energy cosmic ray air showers", Proc. 29<sup>th</sup> ICRC, Pune, India, Tata Institute of Fundamental Research, eds. B. S. Acharya et al., Vol. 8 (2005) 45.
- [20] T. Antoni et al. - KASCADE collaboration, Nucl. Instr. Meth. A 513 (2003) 429.

- [21] A. Haungs et al. - KASCADE-Grande collaboration, Proc. 22nd Texas Symposium on Relativistic Astrophysics, Stanford, California, 13-17 Dec 2004, TSRA-2004-2414, eConf C041213:2414 (2004).
- [22] <http://www.lofar.org/>
- [23] A. Horneffer et al. - LOPES collaboration, "Radio Detection of Cosmic Rays with LOPES", Proc. of ARENA workshop May 2005, Zeuthen, Germany, Int. J. of Mod. Phys. A (2006), in press.
- [24] S. Buitink et al. - LOPES collaboration, "Electric field influence on the radio emission of air showers", Proc. of 29<sup>th</sup> ICRC, Pune, India, Tata Institute of Fundamental Research, eds. B. S. Acharya et al., Vol. 6 (2005) 333.
- [25] H.R. Allan, Prog. in Element. Part. and Cos. Ray Phys., Vol. 10 (1971) 171.
- [26] R. Glasstetter et al. - KASCADE-Grande collaboration, Proc. of 28<sup>th</sup> ICRC, Tsukuba, Japan, Universal AScademy press Tokyo, eds. T. Kajita et al., (2003) p.781.
- [27] R. Glasstetter et al. - KASCADE-Grande collaboration, "Shower Size Reconstruction at KASCADE-Grande", Proc. of 29<sup>th</sup> ICRC, Pune, India, Tata Institute of Fundamental Research, eds. B. S. Acharya et al., Vol. 6 (2005) 233.
- [28] J. van Buren et al. - KASCADE-Grande collaboration, "Muon Size Spectrum measured by KASCADE-Grande", Proc. of 29<sup>th</sup> ICRC, Pune, India, Tata Institute of Fundamental Research, eds. B. S. Acharya et al., Vol. 6 (2005) 301.
- [29] A. Horneffer, "Measuring Radio Emission from Cosmic Ray Air Showers with LOPES", PhD thesis, Rheinische Friedrich-Wilhelms-Universität Bonn, Germany (2006).
- [30] D. Ardouin et al. - CODALEMA Collaboration, "Features of Radio-Detected Air Showers with CODALEMA", ASTRO-PH 0510170 (2005).